Original Article

Overexpression of *MRPL19* in predicting poor prognosis and promoting the development of lung adenocarcinoma

Dong Wei[1,2], Daqiang Sun[3], Rafael Sirera[4], Muhammad Zubair Afzal[5], Tracy L. Leong[6], Xin Li[3], Yuhang Wang[1]

[1]Graduate School, Tianjin Medical University, Tianjin, China; [2]Department of Thoracic Surgery, the First Affiliated Hospital of Hebei North University, Zhangjiakou, China; [3]Department of Thoracic Surgery, Tianjin Chest Hospital of Nankai University, Tianjin, China; [4]Department of Biotechnology, Universitat Politècnica de València, València, Spain; [5]Hematology-Oncology, Dartmouth-Hitchcock Medical Center, Medical Center Dr., Lebanon, NH, USA; [6]Department of Respiratory Medicine, Austin Hospital, Heidelberg, Victoria, Australia

Contributions: (I) Conception and design: D Wei, D Sun; (II) Administrative support: D Sun; (III) Provision of study materials or patients: D Wei; (IV) Collection and assembly of data: D Wei, X Li, Y Wang; (V) Data analysis and interpretation: D Wei, Y Wang; (VI) Manuscript writing: All authors; (VII) Final approval of manuscript: All authors.

Correspondence to: Daqiang Sun, MD. Department of Thoracic Surgery, Tianjin Chest Hospital of Nankai University, No. 261, Taierzhuang South Road, Jinnan District, Tianjin 300000, China. Email: sdqmd@163.com.

Background: Mitochondrial ribosomal protein L19 (*MRPL19*) is a member of the mitochondrial ribosomal protein (MRP) family. MRPs have a role in the progression of many cancers. However, the role of *MRPL19* in lung adenocarcinoma (LUAD) is yet unknown.

Methods: The Cancer Genome Atlas (TCGA) and Gene Expression Omnibus (GEO) datasets, real-time polymerase chain reaction, and immunohistochemistry (IHC) were used to assess *MRPL19* expression and clinical relevance. Gene Expression Profiling Interactive Analysis (GEPIA) and the online Kaplan-Meier (KM) Plotter database were used to determine the prognostic significance. Through use of LinkedOmics, genes that were coexpressed with *MRPL19* and its regulators were identified. The biological roles of *MRPL19* were investigated through R-implemented packages and RNA interference. The Tumor Immune Estimation Resource (TIMER) was employed to assess the connection between *MRPL19* expression and infiltrated immune cells in LUAD.

Results: *MRPL19* expression in LUAD was upregulated and was correlated with lymph node metastasis, differentiation level, and tumor status. *MRPL19* was prognostic and associated with poor prognosis. Functional network analysis revealed that *MRPL19* may be associated with the cell cycle, cell adhesion molecules, spliceosome, and T-helper cell differentiation and was regulated by several microRNA and the E2F family. The gene set enrichment analysis (GSEA) and protein-protein interaction (PPI) network indicated that *MRPL19* was correlated with cancer proliferation signaling pathways. The immune infiltration analysis revealed a correlation between *MRPL19* expression and the extent of B cells, $CD4^+$ T cells, and dendritic cells' infiltration in LUAD. Additionally, *MRPL19* knockdown in LUAD cells substantially reduced cell growth, migration, and invasion of malignant cells.

Conclusions: The poor prognosis and immunological infiltration in LUAD were significantly associated with *MRPL19*, which may have pro-oncogenic effects on the disease.

Keywords: Mitochondrial ribosomal protein L19 (*MRPL19*); lung adenocarcinoma (LUAD); prognosis; immune infiltration; development

Submitted May 12, 2023. Accepted for publication Jul 07, 2023. Published online Jul 19, 2023.
doi: 10.21037/tlcr-23-306
View this article at: https://dx.doi.org/10.21037/tlcr-23-306

Introduction

Lung cancer is still the most common cause of death globally, with non-small cell lung cancer (NSCLC) accounting for 85% of these deaths. Lung adenocarcinoma (LUAD), which accounts for around 40% of lung cancers, is now the most prevalent kind of NSCLC, and its incidence is still increasing (1,2). Surgical procedures, radiotherapy, chemotherapy, immunotherapy, molecularly targeted treatment, or combinations of these modalities are currently used to manage lung cancer (3). Although some patients with positive driver genes, such as *EGFR*, *ALK*, *RET*, *BRAF*, *ROS1*, *NTRK*, *MET* and *KRAS* (4), can achieve some benefits from targeted treatment, the 5-year survival rate is still poor and individuals still encounter problems of tumor gene mutation and drug resistance. To improve the prognosis, it is vital to identify any probable genetic alterations and pathways in the development of lung cancer.

Mitochondrial ribosomal proteins (MRPs) are encoded by nuclear genes and then translated by 80S cytoplasmic ribosomes. Following particular targeting and sorting, MRPs are imported into the mitochondria and then are assembled into mitochondrial ribosomes (5). MRPs are involved in the growth of several malignancies and can be employed as diagnostic and therapeutic markers in some cases (6), such as *MRPL13* promoting the proliferation of NSCLC and being used as a potential target for the immunotherapy of NSCLC (7), *MRPL42* promoting the proliferation and migration of LUAD cells by being activated by YY1 (8), *MRPL35* knockdown weakening the colorectal cancer cell proliferation and inducing apoptosis and inhibiting the tumor growth (9). Mitochondrial ribosomal protein L19 (*MRPL19*) is a protein-coding gene, located on chromosome 2p12 and encodes the protein components of the large mitochondrial ribosome subunit that has a sedimentation coefficient of 39S. *MRPL19* knockdown can decrease oxygen deprivation/reperfusion (OGDR)-induced apoptosis in the neuroblastoma cell line SK-N-BE (2) and additionally is a probable target for the therapy of cerebral ischemia-reperfusion damage (10). *MRPL19* has been identified as a diffuse non-Hodgkin lymphoma (DNHL)-associated gene by a transcriptome-wide association study (TWAS) although the potential biological mechanism has not been verified (11). For type I or II endometrial malignancies (12), melanoma (13) and pancreatic carcinoma (14), *MRPL19* has also been employed as an intrinsic reference gene. Furthermore, neither the expression nor medical importance of *MRPL19* in LUAD has been investigated, and whether *MRPL19* has functions similar to other MRPs remains unclear.

Using information from the Gene Expression Omnibus (GEO) and The Cancer Genome Atlas (TCGA) databases, we examined *MRPL19* expression in LUAD and its potential predictive significance. Additionally, we investigated *MRPL19*'s role in cancer immunity and clarified the underlying biological processes (BPs) and important pathways underscoring the relationship between *MRPL19* and LUAD. We further employed immunohistochemistry (IHC) staining to confirm the expression of *MRPL19* and its possible prognostic significance in LUAD and conducted *in vitro* cell experiments to clarify the functions of *MRPL19* that promote the development of LUAD. We present this article in accordance with the MDAR and REMARK reporting checklists (available at https://tlcr.amegroups.com/article/view/10.21037/tlcr-23-306/rc).

Highlight box

Key findings

- *MRPL19* expression in lung adenocarcinoma (LUAD) was upregulated, and the high expression of *MRPL19* was found to indicate the poor prognosis of patients with LUAD. *MRPL19* may correlate with some cancer proliferation signaling pathways and tumor immune infiltration.

What is known and what is new?

- Our article verified that high *MRPL19* expression was associated with the poor prognosis of LUAD, and may have pro-oncogenic effects on the disease.
- This study was the first to report the expression of *MRPL19* in relation to LUAD and the possible functions.

What is the implication, and what should change now?

- In spite of our findings, the molecular pathways of *MRPL19* in LUAD remain unclear, and further research is still required to confirm the probable biological mechanisms of *MRPL19* in the development of LUAD.

Methods

Data acquisition and preprocessing

For this investigation, TCGA (https://portal.gdc.cancer.gov/) and GEO (https://www.ncbi.nlm.nih.gov/geo/) were used to retrieve all malignant cell data. TCGA-ALL provided the RNA sequencing information for 11,093 pan-cancer specimens, whereas TCGA-LUAD provided the information for 535 LUAD cases and 59 healthy lung

tissue samples. To make it easier to compare these data with chip data, TCGA standardizes all raw RNA-sequencing data in terms of fragments per kilobase million (FPKM) through log2 (FPKM+1), which was then converted to the form of transcripts per million (TPM) for this study. The microarray and RNA sequencing data for LUAD were acquired from the GEO database and included GSE21933 (n=11) and GSE33532 (n=60). Data from the 2 datasets were normalized with the R package "preprocessCore" (The R Foundation of Statistical Computing, Vienna, Austria) and log2 conversion and then processed with the "limma" package. After processing, the GEO dataset included 51 LUAD specimens and 20 healthy lung tissue specimens. The Cancer Cell Line Encyclopedia (CCLE) dataset (available at https://sites.broadinstitute.org/ccle) was employed to construct the cell line expression matrix for pan-cancer (15). A total of 56 LUAD specimens and 55 surrounding nontumor specimens were obtained from patients with LUAD undergoing surgery at the First Affiliated Hospital of Hebei North University. Hematoxylin and eosin staining, paraffin embedding, and plating of samples onto a human tissue microarray (TMA) were all completed. The study was conducted in accordance with the Declaration of Helsinki (as revised in 2013). The study was approved by the Ethics Committee of the First Affiliated Hospital of Hebei North University (No. W2023012). None of the patients were subjected to radiotherapy or chemotherapeutics before operation and all of the participants signed an informed consent. The HBE135-E6E7 healthy lung cell line [American Type Culture Collection (ATCC) CRL-2741] and the LUAD cell lines NCI-H1299 (CVCL-0060), A549 (CVCL-0023), and 95-D (ATCC CL-0011) were examined in this study.

Differential expression and survival analysis based on public databases

The analysis of differential *MRPL19* gene expression between LUAD samples and adjacent nontumor samples was completed using R software, and the outcomes were displayed using the "ggplot2" package. The expression differences of *MRPL19* between pan-cancer samples and their adjacent nontumor samples accordingly, and the expression of *MRPL19* in pan-cancer cells were also analyzed with the above-mentioned method. *MRPL19* expression in cancer subgroups was examined based on clinicopathological features using UALCAN (http://ualcan.path.uab.edu/), which includes TCGA level 3 RNA-sequencing and medical data from 31 kinds of tumors (16). The Kaplan-Meier (KM) plotter (https://kmplot.com/analysis/) online database and Gene Expression Profiling Interactive Analysis (GEPIA) (http://gepia.cancer-pku.cn/) web tools were employed to create a survival curve and to evaluate the impact of *MRPL19* on the prognosis of LUAD. The median *MRPL19* expression was used as a threshold, while overall survival (OS) was used as the end point to plot the survival curve.

RNA extraction and real-time quantitative polymerase chain reaction (RT-qPCR) analysis

The manufacturer's recommendations were followed in conducting the RNA isolation and RT-qPCR tests. TRIzol reagents (3101-100; Pufei Biotechnology, Shanghai, China) were used to obtain total RNA, and a Moloney murine leukemia virus reverse transcriptase kit was used to reverse-transcribe the extracted total RNA into complement DNA (cDNA; M1705; Promega Corp., Shanghai, China). SYBR Premix Ex Taq (DRR041B; Takara Bio, Kusatsu, Japan) was adopted in RT-qPCR to identify gene expression. Primers (RiboBio, Guangzhou, China) were used to target *MRPL19* and its endogenous control ACTB (beta actin). The *MRPL19* expression in several cell lines was assessed with ΔCt, and the effectiveness of *MRPL19*'s subsequent gene knockdown in comparison to the control group was expressed as $2^{-\Delta\Delta Ct}$. The primers used in this study were the following: MRPL19 (F: 5'-GAGAAACGGCTGGATGATAGC-3'; R: 5'-AGGCTCTTGTACTACTGGCTTC-3'); and ACTB (F: 5'-GCGTGACATTAAGGAGAAGC-3'; R: 5'-CCACGTCACACTTCATGATGG-3').

IHC

The expression of *MRPL19* was analyzed in TMA by IHC. Primary MRPL19 antibody was diluted to 1:100 (16517-1-AP; Proteintech Corp., Chicago, USA). The UltraSensitive SP IHC Kit (mouse/rabbit; KIT-9720; Fuzhou Maixin Biotech Co., Ltd., Fuzhou, China) was employed as secondary antibody for visualization. Counterstaining was performed using hematoxylin. Two experienced independent pathologists who were not informed of the patient's situation evaluated the IHC data. Staining was scored by the intensity of the positive staining (0, negative; 1, weak; 2, moderate; and 3, strong) multiplied by the stained regions (0, negative; 1, 1–25%; 2, 26–50%;

3, 51–75%; and 4, 76–100%). By analyzing the receiver operating characteristic (ROC) curve, the best threshold was identified.

Coexpression gene assessment

The LinkedOmics database (http://www.linkedomics.org/login.php) is an online tool for examining multidimensional data sets related to TCGA (17). A total of 515 high-throughput sequencing messenger mRNA (Hiseq-mRNA) data sets of LUAD from the LinkedOmics Database were employed to assess *MRPL19* coexpressed genes via Pearson correlation coefficients, the results of which were displayed in volcano plots and heatmaps. GEPIA2 (http://gepia2.cancer-pku.cn/) was employed to construct the survival map of the 50 major genes positively and negatively correlating with *MRPL19*.

Gene Ontology (GO) and Kyoto Encyclopedia of Genes and Genomes (KEGG) mechanism enrichment assessment

A threshold of |R-statistic| >0.2 was used to identify genes that were coexpressed with *MRPL19*. The "clusterProfiler" package in R was employed to examine the GO and KEGG enrichment assessment of these obtained co-expression genes. The GO enrichment study included BPs, cellular components (CCs), and molecular functions (MFs). The "ggplot2" package in R was employed to display the findings.

Gene set enrichment analysis (GSEA)

Gene ranking was completed on the coexpression genes of *MRPL19* according to |R-statistic|. GSEA was conducted to investigate the underlying biological pathway of *MRPL19* in the development of LUAD. To this end, the packages "clusterProfiler" and "org.Hs.eg.db" were used on the hallmark gene sets from the GSEA's official website. For each experiment, a total of 1,000 cycles of gene permutations were run to identify the enriched mechanisms. To identify significantly the enriched gene sets and mechanisms, false-discovery rate (FDR)-modified P values and normalized enrichment scores (NESs) were calculated.

Construction of a protein-protein interaction (PPI) network

An effective tool for functional enrichment, interactome assessment, gene annotation, and membership search is provided on Metascape website (http://metascape.org/) (18). Those *MRPL19* coexpression genes that met the threshold of |R-statistic| >0.4 and a P value <0.05 were selected. A PPI network was constructed using these acquired coexpressed genes with the aid of Metascape, and the main pathways were analyzed.

The prediction of upstream regulators

In total, 515 Hiseq-mRNA datasets of LUAD from the LinkedOmics database were examined. To conduct kinase-target enrichment, microRNA (miRNA)-target enrichment, and transcription factor-target enrichment using GSEA, the LinkedOmics LinkInterpreter module was used with a criterion of an FDR-adjusted P value <0.05

Immune infiltration analysis

The Tumor Immune Estimation Resource (TIMER) database (19) from TCGA provides a comprehensive means for systematically examining immune infiltrates in types of malignancy (https://cistrome.shinyapps.io/timer/) with a deconvolution technique. Using the "Gene" module, this study investigated the link between the expression of *MRPL19* and the LUAD purity and the quantity of tumor-infiltrating immune cells (TIICs). The SCNA (somatic copy number alterations) module was employed to clarify the connection among *MRPL19* copy number variations (CNVs) and the degree of immune cell infiltration. The relationship between *MRPL19* expression and immune cell infiltration level with prognosis was investigated using the "Survival" module.

Lentivirus short hairpin RNA and transfection

Control small interfering RNA (siRNA) and short hairpin RNA (shRNA) were obtained from Generay (Shanghai, China) for the interference sequence targeting of *MRPL19*. Using the GV115 vector, siRNA control and siRNA-*MRPL19* were transfected into the A549 and H1299 cell lines (GeneChem Inc., Shanghai, China). The target sequence of shRNA *MRPL19* was 5'TGGATGATAGCTTGCTATA-3'.

Western blotting

Cells were lysed in radioimmunoprecipitation assay (RIPA) lysis buffer on ice after being rinsed twice with

phosphate-buffered saline (PBS). Sodium dodecyl sulfate (12%)-polyacrylamide gel electrophoresis (SDS-PAGE) was employed to disassociate and separate all the proteins according to their molecular masses. The protein amount was detected with a bicinchoninic acid (BCA) reagent kit (AS1086; Aspen Technology, Inc., Shanghai, China). SDS-PAGE gels were transferred onto polyvinylidene fluoride (PVDF) membranes. Total protein was identified using Western blotting with anti-MRPL19 (1:3,000; 16517-1-AP; Proteintech) and anti-β-Actin (1:10,000; TDY051; TDY Biotech Corp., Beijing, China). After incubation with the second antibodies (goat anti-rabbit: 1:10,000; AS1107; Aspen Technology, Inc.), proteins were identified using an enhanced chemiluminescence (ECL) detection kit (AS1059; Aspen Technology, Inc.) in accordance with the manufacturer's guidelines.

Celigo cell growth test

96-well plates were seeded with shCtrl and sh*MRPL19* cells at a density of 1,000–2,000 cells/well depending on the growth rate. Cells were cultured in an incubator (MOC-175-175; Sanyo, Osaka, Japan) with 5% CO_2 at 37 ℃. Cells were screened every day for 5 days to acquire images using a Celigo full-field cell scan analyzer (Celigo; Nexcelom Bioscience, Shenzhen, China) and the number of cells was calculated with a cell counter (Auto1000; Nexcelom Bioscience). Cell proliferation curves were plotted after 5 consecutive days of counting.

Colony formation test

The capability of cells to grow was evaluated with the colony formation test. Experimental and control cells were added and cultivated in 6-well soft agar mixture plates at 1,000 cells per well for 7 days. Following crystal violet (CB0331; Sangon Biotech, Shanghai, China) staining, the colonies with greater than 50 cells that survived were counted. Three separate cycles of the trials were performed.

Apoptosis assay

Six-well plates (no less than 5×10^5 cells per well) each were seeded with experimental and control cells. According to the manufacturer's recommendations, Annexin V-APC (88-8007; eBioscience, San Diego, USA) staining was used to analyze apoptosis, and flow cytometry (C6 PLUS; BD, New Jersey, USA) was used to determine the rate of apoptosis in the cells.

MTT assay

shCtrl and sh*MRPL19* cells were multiplied at a concentration of 2×10^3 cells per well in 96-well plates. On days 1, 2, 3, 4, and 5, a total of 20 μL of MTT (methyl thiazolyl tetrazolium) (5 mg/mL) was administered to every well. Following a further 4 hours of cultivation, 100 μL of dimethyl sulfoxide was administered to each well. With a microplate reader (M2009PR; Tecan Infinite, Mannedorf, Switzerland), the concentration of every well at 490 nm [optical density (OD) 490] was determined following reduced-speed shaking for 5 min. Curves for cell growth were drawn.

Cell migration and invasion assay

Transwell tests were used for examinations on migration and invasion. For 48 hours, cells were transfected with shCtrl or sh*MRPL19*. Transfected NCI-H1299 cells were then implanted at a density of 5×10^4 cells, and A549 cells were transfected at a concentration of 1×10^5 cells in 24-well Transwell chambers with 8-μm-thick polycarbonate membrane (Corning, New York, USA). After 100 μL of serum-free medium was added to the top chamber and 600 μL of media with 30% fetal bovine serum was added to the bottom chamber, cells were cultivated at 37 ℃ for 16 hours to test for migration. Cotton swabs were used to eliminate cells from the filter's top surface, while migrating cells that adhered to the membrane's bottom surface were preserved in 4% paraformaldehyde solution and subjected to 0.5% crystal violet stain. To calculate the number of cells, 9 random selection microscope fields (×200) were chosen. A Matrigel covering was introduced to the polycarbonate membrane for invasion testing, and the experiments were conducted using the same procedure. Three separate repetitions of the tests were conducted.

Statistical analysis

R software (version 3.6.3), SPSS 20.0 (IBM Corp., Armonk, New York, USA), and GraphPad Prism 8.1.1 (GraphPad Software, Inc., San Diego, CA, USA) were used for statistical analyses. The association between *MRPL19* expression and the clinical characteristics of LUAD was evaluated using the chi-squared (χ^2) test. The comparison between the 2 cohorts (the experimental group and the

control) was completed with the Mann-Whitney test and Student's *t*-tests. To determine the survival time in the *MRPL19* low- and high-expression groups, KM analysis was performed. The IHC score ≤3 was considered as low expression while >3 was the high expression. The cutoff value was obtained by ROC curve. The relationship between survival time, clinical prognostic markers, and *MRPL19* expression was examined using univariate and multivariate Cox regression models. The relation between the degree of immune cell infiltration and *MRPL19* expression was examined using the partial Spearman correlation coefficient. Statistical significance was recognized as a 2-sided P<0.05.

Results

High expression of MRPL19 in LUAD

By employing pan-cancer information from TCGA database, the changes in *MRPL19* expression at the transcriptional level were assessed in 33 different kinds of cancers. In LUAD, *MRPL19* mRNA expression was substantially high (*Figure 1A*). The CCLE database indicated that *MRPL19* mRNA was elevated in LUAD and other cancer cells at the cellular level (*Figure 1B*). Expression differences between LUAD samples and adjacent nontumor samples were analyzed using TCGA-LUAD data, which also indicated that *MRPL19* mRNA expression was substantially elevated in LUAD compared to neighboring healthy tissues (*Figure 1C*). Moreover, the upregulated levels of *MRPL19* mRNA in LUAD were also validated in the GEO database data sets (*Figure 1D*). RT-qPCR assessment was conducted to evaluate the relative levels of mRNA among healthy lung epithelial cells (HBE135-E6E7) and several LUAD cell lines, including NCI-H1299, A549, and 95-D, in order to further confirm this result. NCI-H1299, A549, and 95-D cells had higher levels of *MRPL19* mRNA than did the HBE135-E6E7 cell line (*Figure 1E*). The outcomes also showed that the NCI-H1299 and A549 cell lines had higher levels of *MRPL19* mRNA than did the 95-D cell line.

For the *MRPL19* knockdown assays, the NCI-H1299 and A549 cell lines were used. *MRPL19* expression at the protein level was much higher in the IHC results of 56 LUAD specimens than of the 55 neighboring healthy samples (P<0.01; *Figure 1F,1G*). Upregulation of *MRPL19* was shown at both the transcription and protein level through subgroup examination of multiple clinicopathological features of TCGA-LUAD specimens using the UALCAN database. *MRPL19* expression at the transcription level was substantially higher in LUAD than in healthy controls in the subgroup investigation depending on gender, age, ethnicity, and cancer stage (*Figure 2A-2E*). Additionally, upregulation of *MRPL19* at the protein level was also demonstrated in LUAD in the subgroup evaluation depending on gender, race, tumor grade, and stage (*Figure 2F-2J*).

MRPL19 overexpression was correlated with poor prognosis in individuals with LUAD

To evaluate the impacts of *MRPL19* expression on LUAD prognosis, KM survival curves based on OS were constructed to evaluate the relation between *MRPL19* expression and survival using LUAD data sets with available survival information. The cohort with aa higher expression of *MRPL19* had a substantially shorter OS [hazard ratio (HR) =1.5; log rank P=0.0059] than did the reduced expression group according to KM analysis of the GEPIA TCGA-LUAD datasets (*Figure 3A*). Furthermore, KM survival curve examination employing KM Plotter GEO datasets from the KM plotter further confirmed the association between elevated *MRPL19* expression and poor survival (HR =1.45; log rank P=0.0029; *Figure 3B*). Additionally, IHC staining in TMA samples confirmed these findings (P=0.0004; *Figure 3C*). The relationship between *MRPL19* expression in LUAD and clinicopathological traits was also examined using TMA samples. According to the findings, there was a substantial association between MRPL19 expression and OS status (living *vs.* dead: P=0.003), differentiation grade (P=0.046), and lymph node metastasis (positive *vs.* negative: P=0.026) (*Table 1*). To confirm the prognostic efficacy of *MRPL19* in LUAD, univariate and multivariate Cox regression assessment was conducted. The findings revealed that that overexpression of *MRPL19* was an independent prognostic variable in LUAD (HR =2.822, 95% CI: 1.113–7.159; P=0.029; *Table 2*).

MRPL19 coexpression genes in LUAD

The utility of gene coexpression analysis in examining the roles of certain genes has previously been established. According to various research, coexpressed genes functioned in comparable BPs. Therefore, an analysis of *MRPL19* coexpression genes was performed in LUAD. The LinkedOmics function module was used to analyze *MRPL19* coexpression genes in LUAD, and all coexpression genes are

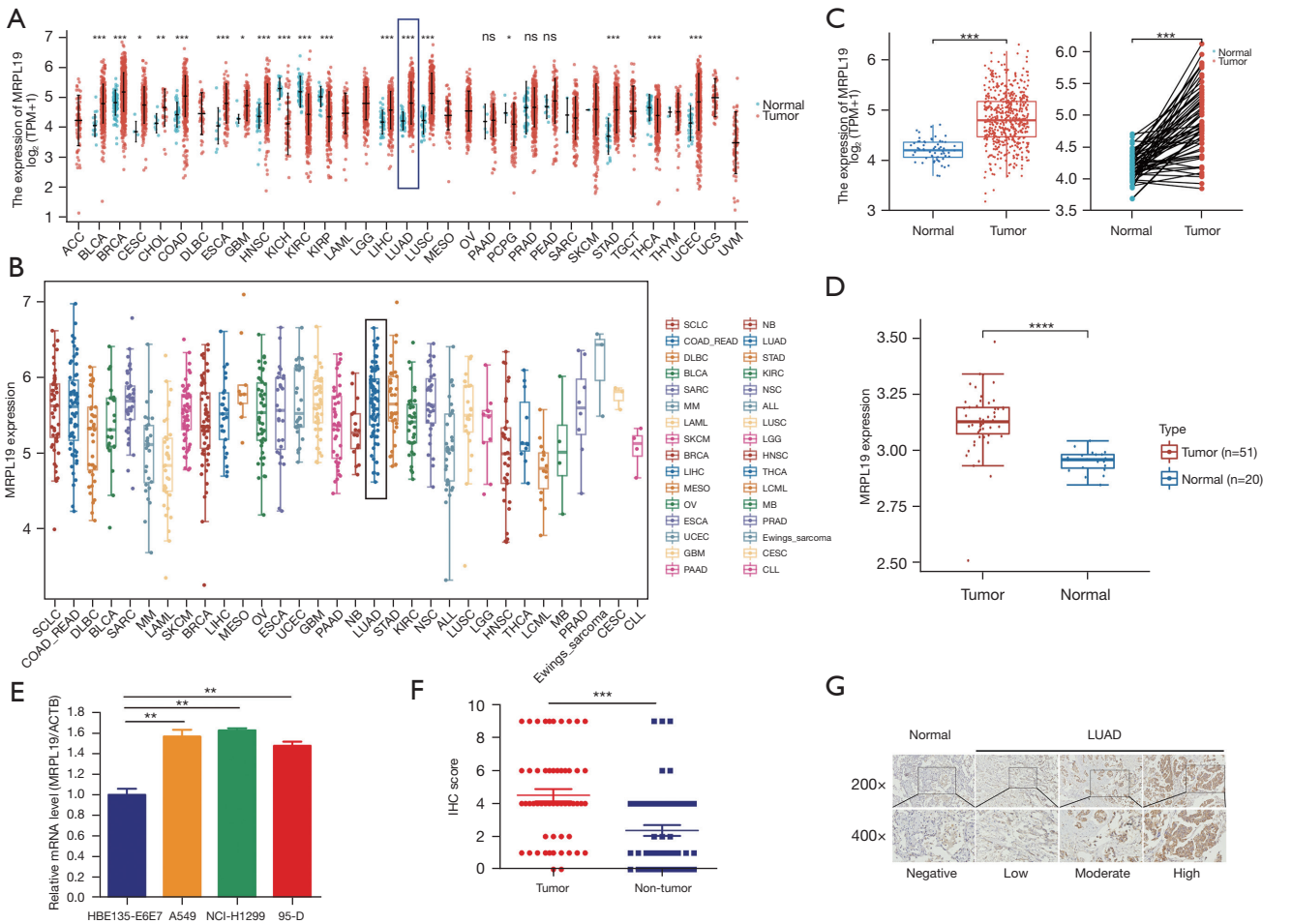

Figure 1 Expression of *MRPL19* in LUAD. (A) The mRNA expression level of *MRPL19* in the pan-cancer data from TCGA database. (B) The expression of *MRPL19* mRNA in different tumor cells. (C) Differential expression of *MRPL19* mRNA from TCGA database. (D) Differential expression of *MRPL19* mRNA from GEO database. (E) Expression of *MRPL19* mRNA in different LUAD cell lines and normal lung epithelial cell lines. (F) Expression of *MRPL19* protein from clinical samples. (G) Typical IHC staining images of *MRPL19* in normal lung tissue and LUAD tissues (IHC staining method. Magnification ×200 and ×400). *, P<0.05; **, P<0.01; ***, P<0.001; ****, P<0.0001; ns, not significant. *MRPL19*, mitochondrial ribosomal protein L19; TPM, transcripts per million; ACTB, beta actin; IHC, immunohistochemistry; LUAD, lung adenocarcinoma; TCGA, The Cancer Genome Atlas; GEO, Gene Expression Omnibus.

presented in a volcano plot (*Figure 4A* and available online https://cdn.amegroups.cn/static/public/tlcr-23-306-1.pdf). The genes coexpressed with *MRPL19* were screened with the threshold of |R-statistic| >0.2 and FDR <0.05. In all 5,434 *MRPL19* coexpression genes were identified, including 1,833 genes with substantial positive correlations and 3,601 genes with substantial negative correlations (available online https://cdn.amegroups.cn/static/public/tlcr-23-306-2.pdf). *Figure 4B,4C* shows the heatmap of the top 50 major genes that were both positively and negatively associated with *MRPL19*. Substantial positive correlations between the expressions of *MTIF2* and *MRPL19* were observed (R=0.612; P=3.05E-50), whereas strong negative correlations between the expressions of *CBX7* and *MRPL19* were observed (R=–0.536; P=1.26E-36). With 31 of these 50 genes having an increased HR (P<0.05), the top 50 substantial genes that were positively linked with *MRPL19* revealed the increased opportunity of having elevated-risk genes in LUAD. Moreover, among the top 50 negatively significant genes, 27 genes had a low HR (P<0.05) (*Figure 4D,4E*).

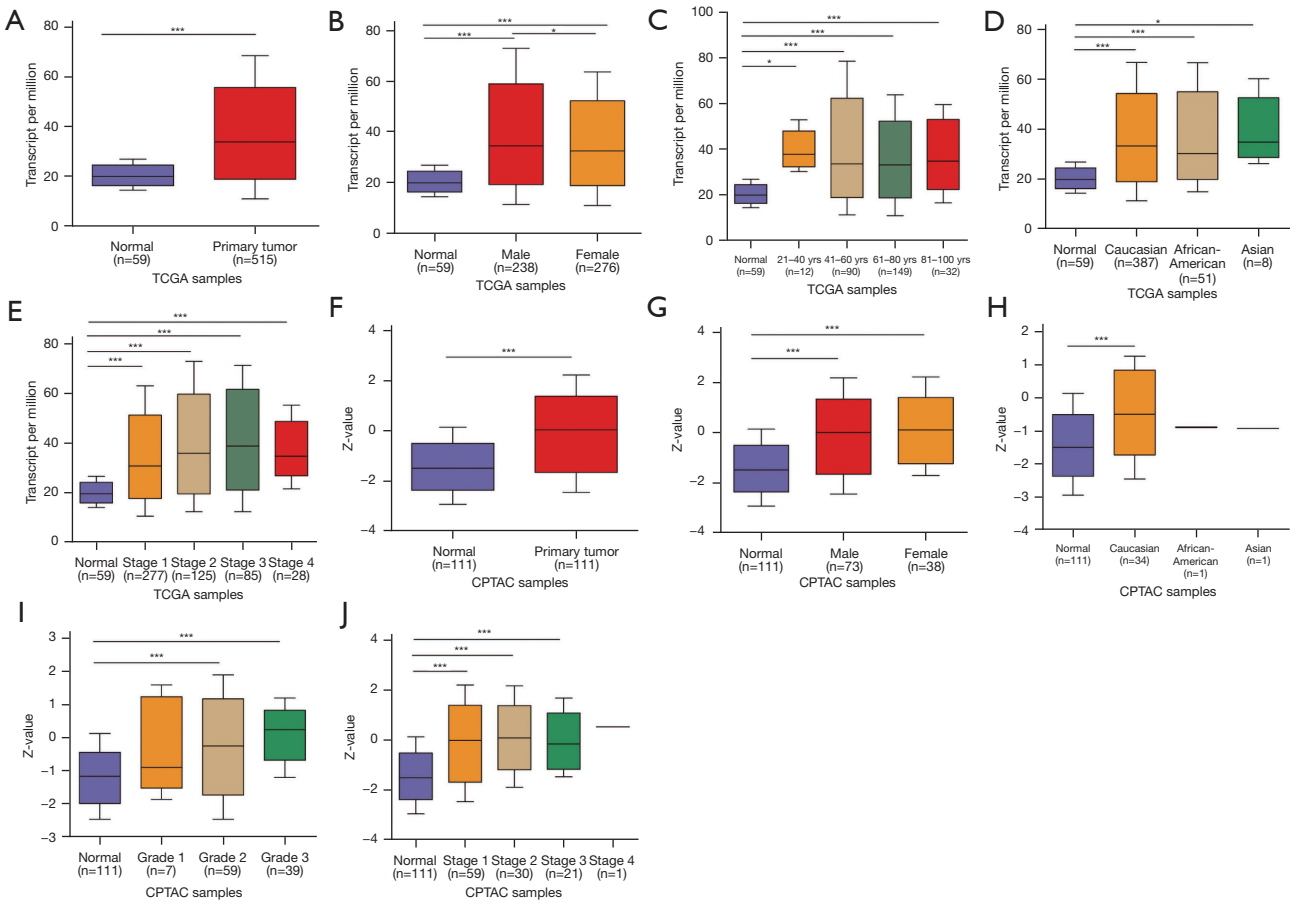

Figure 2 Expression of *MRPL19* in subgroups of patients with LUAD. (A) Relative expression of *MRPL19* mRNA in healthy and LUAD samples. (B) Differential expression of *MRPL19* mRNA between healthy individuals and male or female patients with LUAD. (C) Differential expression of *MRPL19* mRNA between healthy individuals of any age and patients with LUAD aged 21–40, 41–60, 61–80, or 81–100 years. (D) Differential expression of *MRPL19* mRNA between healthy individuals and African-American, White, and Asian patients with LUAD. (E) Differential expression of *MRPL19* mRNA between healthy individuals and patients with stages 1–4 LUAD. (F) Relative expression of *MRPL19* protein in healthy and LUAD samples. (G) The differential expression of *MRPL19* protein between healthy individuals and male or female patients with LUAD. (H) The differential expression of *MRPL19* protein between healthy individuals and African-American, White, and Asian patients with LUAD. (I) The differential expression of *MRPL19* protein between healthy individuals and patients with Grade 1–3 LUAD tumor. (J) The differential expression of *MRPL19* protein between healthy individuals and patients with stages 1–4 LUAD. The *t*-test was used to estimate the significance of difference in gene expression levels between groups. *, P<0.05; ***, P<0.001. TCGA, The Cancer Genome Atlas; CPTAC, the Clinical Proteomic Tumor Analysis Consortium; *MRPL19*, mitochondrial ribosomal protein L19; LUAD, lung adenocarcinoma.

Biological significance of MRPL19

To explore the biological relevance of *MRPL19*, GO annotation, KEGG signaling pathway analysis, PPI network, and GSEA were performed on the MRPL19 coexpression genes. The outcomes of GO annotation examination revealed that the coexpressed genes of *MRPL19* at the BP level were primarily enriched in the biogenesis of ribonucleoprotein complexes, chromosome segregation, mitotic nuclear division or differentiation, proliferation, or triggering of immune cells, such as mononuclear cells, leukocytes, and T cells. At the CC level, *MRPL19* coexpressed genes were mainly enriched in chromosomal area, mitochondrial matrix, and MHC (major histocompatibility complex) protein compound,

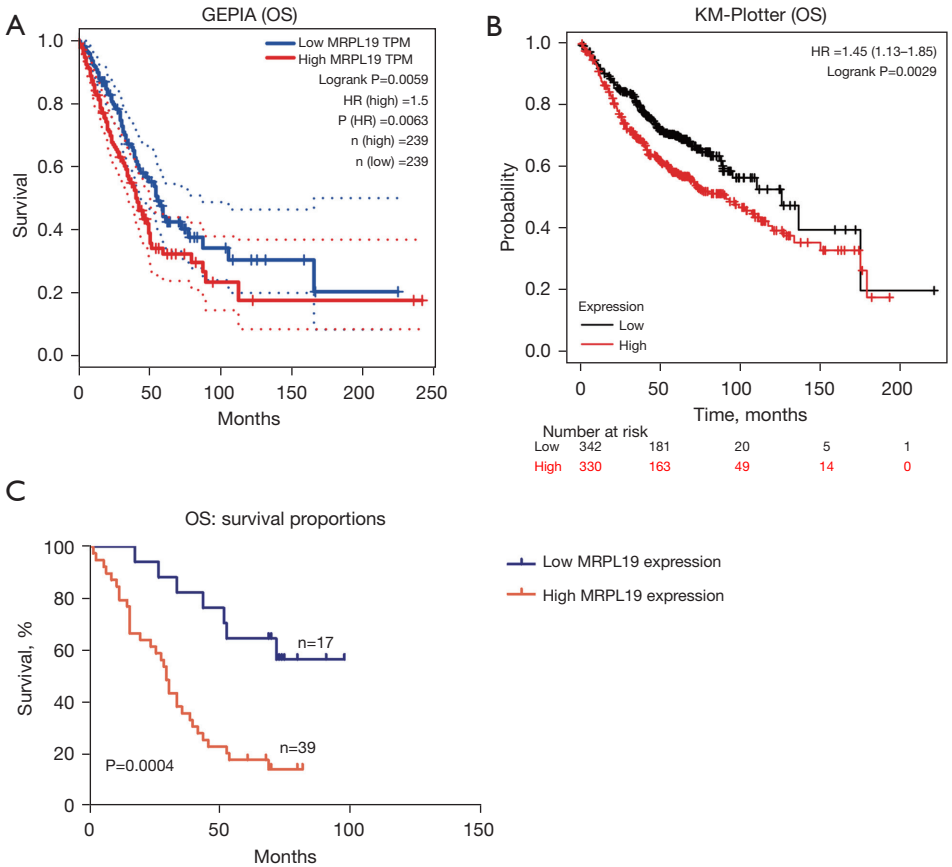

Figure 3 The expression of *MRPL19* was associated with survival outcome. OS based on (A) TCGA-LUAD datasets from GEPIA, (B) the GEO datasets from the Kaplan-Meier plotter, and (C) IHC staining of TMA specimens. GEPIA, Gene Expression Profiling Interactive Analysis; OS, overall survival; TPM, transcripts per million; HR, hazard ratio; KM, Kaplan-Meier; *MRPL19*, mitochondrial ribosomal protein L19; TCGA, The Cancer Genome Atlas; LUAD, lung adenocarcinoma; GEO, Gene Expression Omnibus; IHC, immunohistochemistry; TAM, tissue microarray.

while at the MF level, genes were mainly enriched in ATPase activity, GTPase regulator activity, and catalytic activity acting on DNA (*Figure 5A,5B* and available online https://cdn.amegroups.cn/static/public/tlcr-23-306-3.xlsx). The outcomes of the examination of the KEGG signaling mechanism showed enrichment in the cell cycle, nucleocytoplasmic transport, cell adhesion molecules, spliceosome, and T helper (TH) cell 1, 2, and 17 differentiations. (*Figure 5C,5D* and available online https://cdn.amegroups.cn/static/public/tlcr-23-306-4.xlsx). The PPI network was constructed using Metascape, and 7 key nodes were included in the network (*Figure 5E,5F*). Nineteen main signaling pathways were included in these key nodes, including anaphase promoting complex/cyclosome (APC/C)-mediated degradation of cyclin A, modulation of the DNA metabolic pathway, and mitotic spinal checkpoint (Table S1). The outcomes of GSEA revealed that the *MRPL19* coexpression genes were mainly enriched in the G2M_Checkpoint pathway, MYC_Targets_V1 pathway, MYC_ Targets _V2 pathway, and E2F_Targets pathway (*Figure 5G-5J*).

Upstream regulators of MRPL19 in LUAD

To explore the upstream regulators of *MRPL19* in LUAD, an enrichment analysis of kinases, miRNAs, and transcription factors of *MRPL19* co-expressed genes was performed. Significant miRNAs related primarily to MIR-200A (GTAAGAT), MIR-26A/MIR-26B (TACTTGA), MIR-302C (ATGTTAA), MIR-189 (GTAGGCA), MIR-

Table 1 Association between *MRPL19* expression and clinicopathological characteristics in LUAD

Clinical parameter	Subgroups	Case	*MRPL19* expression		χ^2	P value
			Low	High		
Sex	Male	31	10	21	0.119	0.730
	Female	25	7	18		
Age	≤60 years	29	8	21	0.218	0.640
	>60 years	27	9	18		
Tumor size	≤4 cm	34	13	21	2.541	0.111
	>4 cm	22	4	18		
Pathologic T stage	T1–2	41	16	25	3.581	0.058
	T3–4	14	1	13		
Pathologic N stage	N0	25	11	14	4.939	0.026
	N1–2	30	5	25		
Pathologic M stage	M0	43	14	29	0.094	0.759
	M1	13	3	10		
TNM stage	I–II	23	10	13	3.178	0.075
	III–IV	33	7	26		
Differentiation	1/1–2/2	25	11	14	3.976	0.046
	2–3/3	31	6	25		
OS status	Alive	16	10	6	8.922	0.003
	Dead	40	7	33		

The cutoff value of *MRPL19* expression is 3. *MRPL19*, mitochondrial ribosomal protein L19; LUAD, lung adenocarcinoma; OS, overall survival.

Table 2 The Cox regression analysis of clinicopathologic features with the OS in LUAD

Variable	Univariate analysis			Multivariate analysis		
	P value	HR	95% CI	P value	HR	95% CI
Sex (male *vs.* female)	0.736	0.898	0.482–1.675	–	–	–
Age (≤60 *vs.* >60 years)	0.228	1.467	0.787–2.735	–	–	–
Pathologic T (T1/T2 *vs.* T3/T4)	0.616	0.819	0.376–1.785	–	–	–
Pathologic N (N0 *vs.* N1/N2)	0.005	2.653	1.350–5.216	0.014	2.596	1.214–5.547
Pathologic M (M0 *vs.* M1)	0.002	2.932	1.465–5.867	0.001	4.987	1.960–12.687
TNM (I/II *vs.* III/IV)	0.049	1.909	1.002–3.638	–	–	–
Tumor size (≤4 *vs.* >4 cm)	0.278	0.693	0.357–1.344	–	–	–
Differentiation (1/1–2/2 *vs.* 2–3/3)	0.038	1.998	1.040–3.842	0.037	2.171	1.049–4.490
Expression (low *vs.* high)	0.001	4.048	1.760–9.312	0.029	2.822	1.113–7.159

LUAD, lung adenocarcinoma; OS, overall survival; HR, hazard ratio; CI, confidence interval; TNM, Tumor-Node-Metastasis.

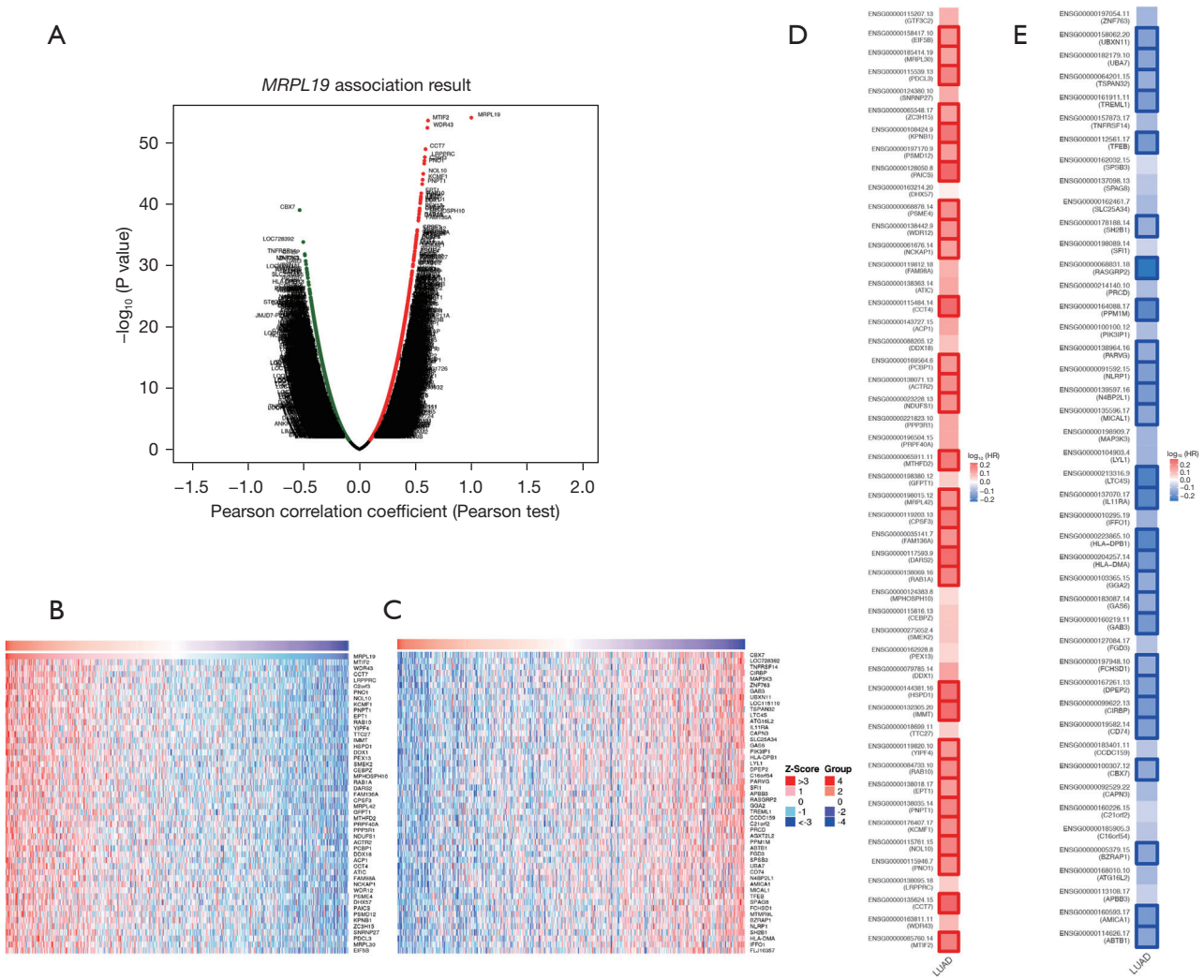

Figure 4 *MRPL19* coexpression genes in LUAD. (A) A volcano plot of the *MRPL19* coexpression genes. Heat maps showing the top 50 genes (B) positively (red) correlated and (C) negatively (blue) correlated with *MRPL19* in LUAD. Survival map of the top 50 genes (D) positively and (E) negatively correlated with *MRPL19* in LUAD. *MRPL19*, mitochondrial ribosomal protein L19; LUAD, lung adenocarcinoma; HR, hazard ratio.

186 (ATTCTTT), and MIR-452 (GAGACTG). No significant kinase was acquired by enrichment analysis of *MRPL19* co-expressed genes. The significant transcription factors related to the co-expressed genes were mainly enriched in E2F transcription factor family, including V$E2F_Q4, V$E2F_Q6, and V$E2F1DP1_01 (*Table 3*).

MRPL19 expression was correlated with immune cell infiltration

According to the findings of the immune infiltration study, B cells (R=–0.224; P=6.18e-07), $CD4^+$ T cells, (R=–0.167; P=2.34e-04), and dendritic cells (R=–0.09; P=4.58e-02) were substantially correlated with *MRPL19* expression (*Figure 6A*). Additionally, B cells, $CD4^+$ T cells, $CD8^+$ T cells, macrophages, neutrophils, and dendritic cells were substantially linked with *MRPL19* CNV (*Figure 6B*). The levels of B cells, dendritic cells, and neutrophil infiltration were substantially connected with the survival of individuals with LUAD, and the reduced level of infiltration indicated poor survival according to the findings of the KM survival curve assessment (*Figure 6C*). The degree of

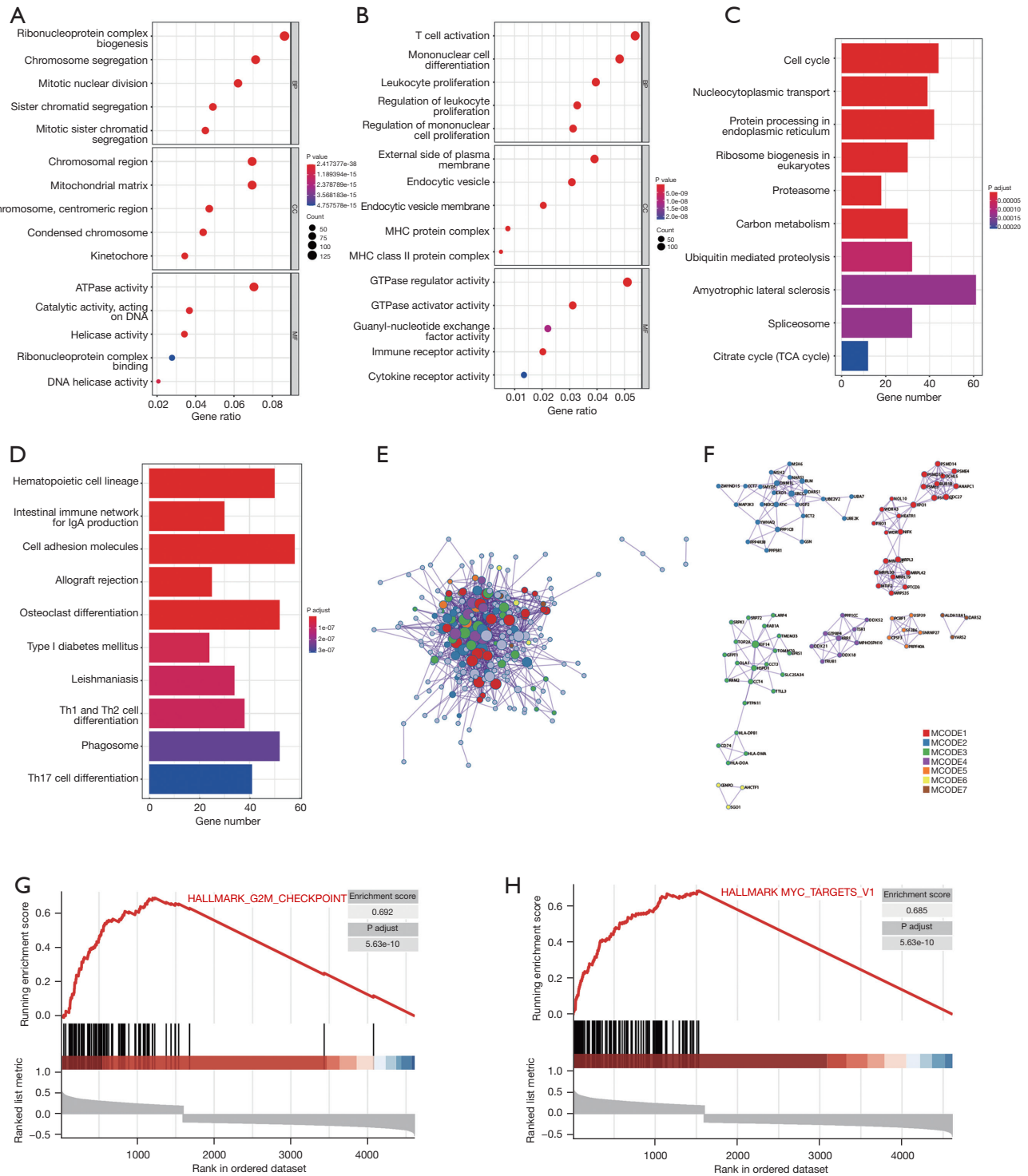

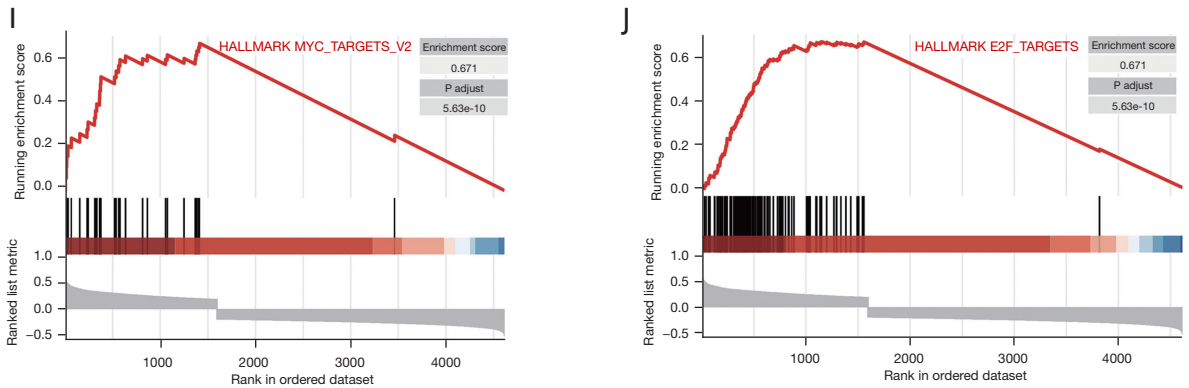

Figure 5 Significantly enriched GO annotations and KEGG pathways of *MRPL19* in LUAD: (A) GO annotations that positively correlated and (B) negatively correlated with *MRPL19* in LUAD. (C) KEGG pathways that positively and (D) negatively correlated with *MRPL19* in LUAD. The GSEA results involving *MRPL19* in LUAD: (E) G2M_Checkpoint signaling pathway. (F) MYC_Targets_V1 signaling pathway, (G) MYC_ Targets _V2 signaling pathway, and (H) E2F_Targets signaling pathway. (I) The PPI network of *MRPL19*. (J) Key nodes in the PPI network. BP, biological process; CC, cellular component; MF, molecular function; MHC, major histocompatibility complex; TCA, tricarboxylic acid cycle; IgA, immunoglobulin A; GO, Gene Ontology; KEGG, Kyoto Encyclopedia of Genes and Genomes; *MRPL19*, mitochondrial ribosomal protein L19; LUAD, lung adenocarcinoma; GSEA, gene set enrichment analysis; PPI, protein-protein interaction.

Table 3 The miRNAs and transcription factor-target networks of *MRPL19* in LUAD

Enriched category	Gene set	Leading edge number	FDR
miRNA target	*GTAAGAT, MIR-200A*	18	0.0074445
	TACTTGA, MIR-26A, MIR-26B	75	0.0099260
	ATGTTAA, MIR-302C	57	0.015385
	GTAGGCA, MIR-189	7	0.016750
	ATTCTTT, MIR-186	65	0.017371
Transcription factor	*V$E2F_Q4*	76	0
	V$E2F_Q6	75	0
	V$E2F1_Q6	87	0
	V$E2F1DP1_01	81	0
	V$E2F1DP2_01	81	0

MRPL19, mitochondrial ribosomal protein L19; LUAD, lung adenocarcinoma; FDR, false-discovery rate.

B-cell infiltration was demonstrated to be an independent prognostic variable in LUAD according multivariate Cox regression (HR =0.045, 95% CI: 0.003–0.782; P=0.033; *Table 4*).

MRPL19 promoted the growth of LUAD cells in vitro

To further elucidate the function of *MRPL19* in LUAD, the target sequence of shRNA MRPL19 was used to silence *MRPL19* expression in LUAD cells. The A549 and H1299 cell lines with a higher expression level of *MRPL19* were selected for further study. RT-qPCR analysis showed that *MRPL19* expression of A549 and H1299 cells transfected with *MRPL19* shRNA was reduced by more than 80%, which was statistically significant compared with the control cohort (*Figure 7A*) (P<0.05). The target sequence of the *MRPL19* shRNA was able to lower *MRPL19* expression at the protein level according to Western blotting data

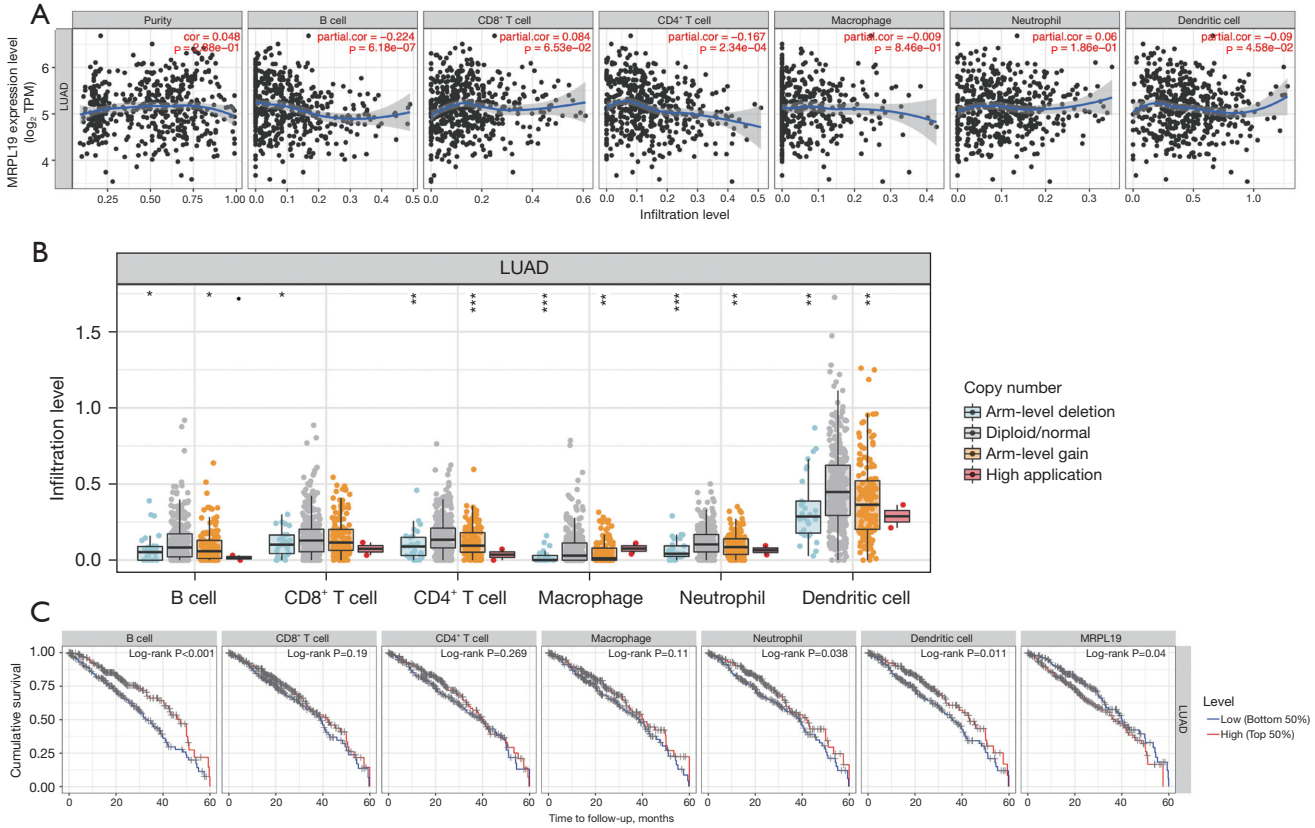

Figure 6 Correlations of *MRPL19* expression with immune infiltration level in LUAD. The association between (A) *MRPL19* expression and (B) *MRPL19* CNV and tumor infiltration immune cells. (C) The correlation of the infiltrating level of tumor immune cells with the OS of patients with LUAD. *, P<0.05; **, P<0.01; ***, P<0.001. *MRPL19*, mitochondrial ribosomal protein L19; TPM, transcripts per million; LUAD, lung adenocarcinoma; CNV, copy number variation; OS, overall survival.

(*Figure 7B*). The findings of the Celigo tests revealed that the A549 and H1299 cell lines' ability to grow was greatly diminished by the removal of *MRPL19* (*Figure 7C*). The MTT tests also revealed that the 2 LUAD cell lines' proliferation was greatly slowed by *MRPL19* knockdown (*Figure 7D*). Colony formation tests revealed that the amount of cell clones in the A549 and H1299 cell lines diminished significantly when *MRPL19* was removed (*Figure 7E*).

Effects of MRPL19 on cell death of LUAD

Flow cytometry was employed to explore the influence of *MRPL19* expression on LUAD cell death. The outcomes indicated that the average proportion of apoptosis of A549 cells in the sh*MRPL19* group was 3.5%, representing a significant increase compared to the shCtrl cohort (*Figure 8A*). The apoptosis rate of H1299 cells in the sh*MRPL19* group was 0.4%, which did not represent a significant change compared to the shCtrl group (*Figure 8B*). No obvious cell apoptosis was observed after *MRPL19* knockdown.

MRPL19 promoted the invasion and migration of LUAD cells

The outcomes of the Transwell migration examination demonstrated that the migration ability of the 2 LUAD cell lines was substantially reduced after removal of *MRPL19* (*Figure 9A*) (P<0.05). The Transwell invasion assessment also indicated that the suppression of *MRPL19* substantially reduced the degree of invasiveness in both selected LUAD cell lines (P<0.05; *Figure 9B*). These results verified that

Table 4 The Cox regression analysis of *MRPL19* expression and immune cell infiltrating level with LUAD prognosis

Variable	Coefficient	HR	95% CI L	95% CI U	P value
Age	0.011	1.011	0.993	1.03	0.238
Sex: male	−0.172	0.842	0.588	1.205	0.346
Race: Black	16.365	12,794,292.853	0	Inf	0.994
Race: White	16.487	14,466,375.88	0	Inf	0.994
Stage 2	0.818	2.267	1.464	3.509	0
Stage 3	0.884	2.42	1.537	3.809	0
Stage 4	1.094	2.987	1.518	5.879	0.002
Purity	0.202	1.224	0.502	2.987	0.656
B cell	−3.091	0.045	0.003	0.782	0.033
$CD8^+$ T cell	−0.667	0.513	0.058	4.506	0.547
$CD4^+$ T cell	1.684	5.39	0.292	99.322	0.257
Macrophage	−0.13	0.878	0.04	19.422	0.934
Neutrophil	−1.343	0.261	0.004	16.328	0.525
Dendritic cell	0.164	1.178	0.276	5.029	0.824
MRPL19	0.257	1.293	0.932	1.794	0.124

MRPL19, mitochondrial ribosomal protein L19; LUAD, lung adenocarcinoma; HR, hazard ratio; CI, confidence interval; L, lower; U, upper; Inf, infinity.

MRPL19 can increase LUAD cell invasion and migration.

Discussion

As a malignant tumor, lung cancer continues to be the leading cause of tumor-related death, representing 18.0% of all cancer-related fatalities (20). LUAD represents 38.5% of all cases and constitutes a greater proportion of lung cancer cases than other histologies (21). Recently, the development of low-dose computer tomography, targeted therapies, and immunotherapy has marginally increased the survival rate of lung cancer (22). The disease progresses in the majority of patients after 6 to 12 months of therapies with epidermal growth factor receptor (EGFR) tyrosine kinase inhibitors (TKIs) due to the appearance of mechanisms of resistance to the original agent (1), so the development of novel LUAD treatment and prognostic targets is now critically essential. According to our findings, LUAD had considerably higher levels of *MRPL19* mRNA expression than did adjacent non-tumor tissue. The protein level likewise showed a similar pattern. Overexpression of *MRPL19* was linked to a poor prognosis in LUAD according to KM analysis. The IHC findings confirmed the hypothesis that the overexpression of *MRPL19* is connected to the OS status. Additionally, univariate and multivariate Cox regression examination pointed to *MRPL19* as being an independent prognostic variable in LUAD. Therefore, the results of this investigation suggest that *MRPL19* may have a potential value in LUAD prognosis, and thus its functions and mechanisms should be scrutinized further.

As *MRPL19* is a member of the MRPs and recent investigations have highlighted its possible function in the biology of malignancy and may be employed as both therapeutic and diagnostic biomarkers. As *MRPL19*'s biological role in LUAD has not yet been examined, we tried to identify the coexpression genes related to *MRPL19* in LUAD and to determine the biological roles of *MRPL19* in this cancer. Strong correlations between the expression of *MTIF2* and *MRPL19* were observed, whereas the expression of *CBX7* and *MRPL19* were strongly inversely correlated. The mitochondrial function of the nuclear-encoded gene *MTIF2* is to execute the translation of proteins encoded by the mitochondrial genome (23). In a 5-fluorouracil (5-FU) treatment *in vivo* model, *MTIF2* overexpression was found suppress hepatocellular carcinoma cell death and immune cell activity by inhibiting tumor-infiltrated dendritic cell

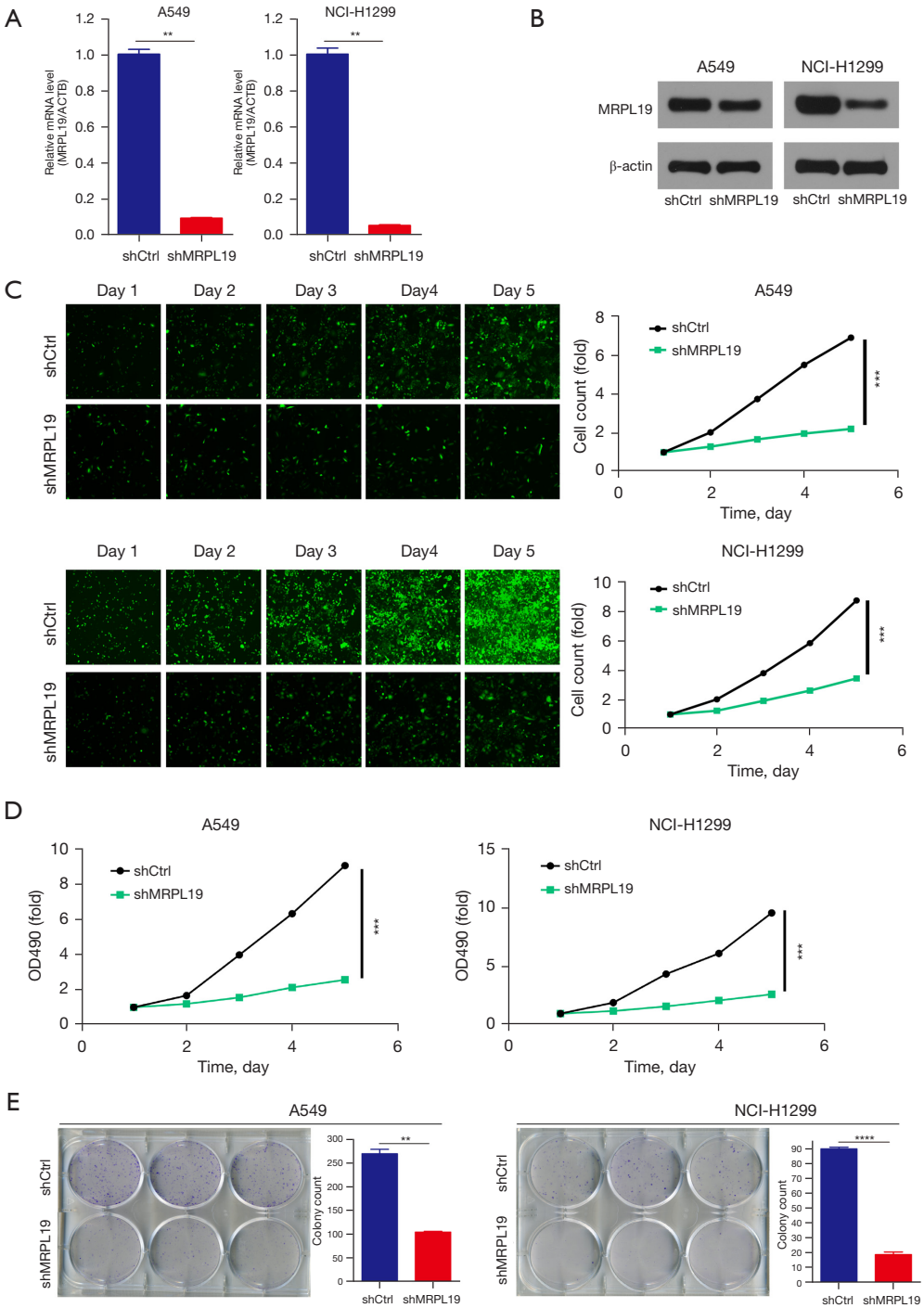

Figure 7 *MRPL19* knockdown suppressed LUAD cell proliferation. (A) RT-qPCR analysis was used to examine the knockdown efficiency of *MRPL19*. (B) Western blotting was performed to analyze protein expression levels of *MRPL19*. Celigo assays (fluorescence staining; magnification ×100) (C), MTT assays (D), and colony formation assays (E) were applied to evaluate cell proliferation (the inoculated cells were cultured in an incubator, and the number of cells in a single clone was observed by ×100 microscope until the number of cells in most of the single clones in the control group was more than 50. The crystal violet staining was performed. The entire culture plate was then photographed. Single clones of 0.3 to 1 mm in size in both groups were counted). **, P<0.01; ***, P<0.001; ****, P<0.0001. *MRPL19*, mitochondrial ribosomal protein L19; ACTB, beta actin; OD, optical density; LUAD, lung adenocarcinoma; RT-qPCR, real-time quantitative polymerase chain reaction; MTT, methyl thiazolyl tetrazolium.

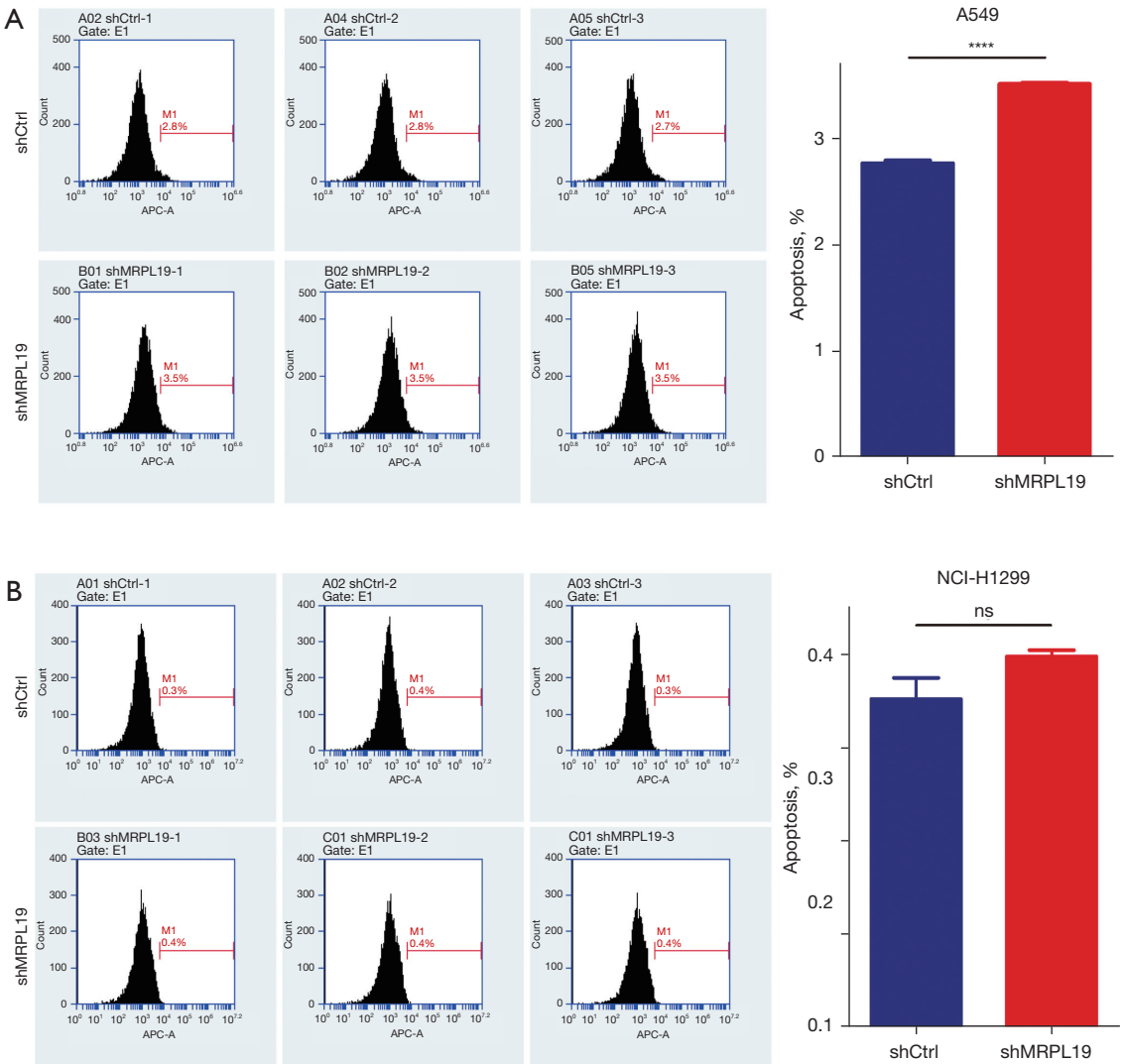

Figure 8 The effect of *MRPL19* knockdown on LUAD cell apoptosis. (A) The apoptosis rate of A549 cells in the sh*MRPL19* group was significantly higher than that of the shCtrl group, but less than 5%. (B) The apoptosis rate of the H1299 cells in the sh*MRPL19* group was less than 5% and had no significant change compared to the shCtrl group. ****, P<0.0001; ns, not significant. *MRPL19*, mitochondrial ribosomal protein L19; APC-A, anaphase promoting complex A; LUAD, lung adenocarcinoma.

maturation (24). *CBX7* is a kind of polycomb protein that is involved in the development of polycomb repressive compound 1, and downregulated *CBX7* expression was reported to be a biomarker of cancer aggressiveness and a poor prognosis (25). *CBX7* downregulation can reduce the sensitivity of bladder cancer to cisplatin (26). Thus, it is suggested that *MRPL19* may have a role in enhancing the development of LUAD. GO annotation, KEGG signaling pathway analysis, PPI network, and GSEA were performed on the *MRPL19* coexpressed genes to obtain more information regarding the biological roles of *MRPL19* in LUAD. The outcomes of the GO annotation demonstrated that the genes coexpressed with *MRPL19* primarily revolved around cell mitosis, energy metabolism, and tumor immunity. KEGG signaling mechanism analysis indicated that the *MRPL19* coexpressed genes may be associated with cell cycle, nucleocytoplasmic transport, cell adhesion molecules, spliceosome, and Th1, Th2, and Th17 cell differentiation. Loss of cell cycle control, which is caused by the lack of equilibrium between oncogenes and

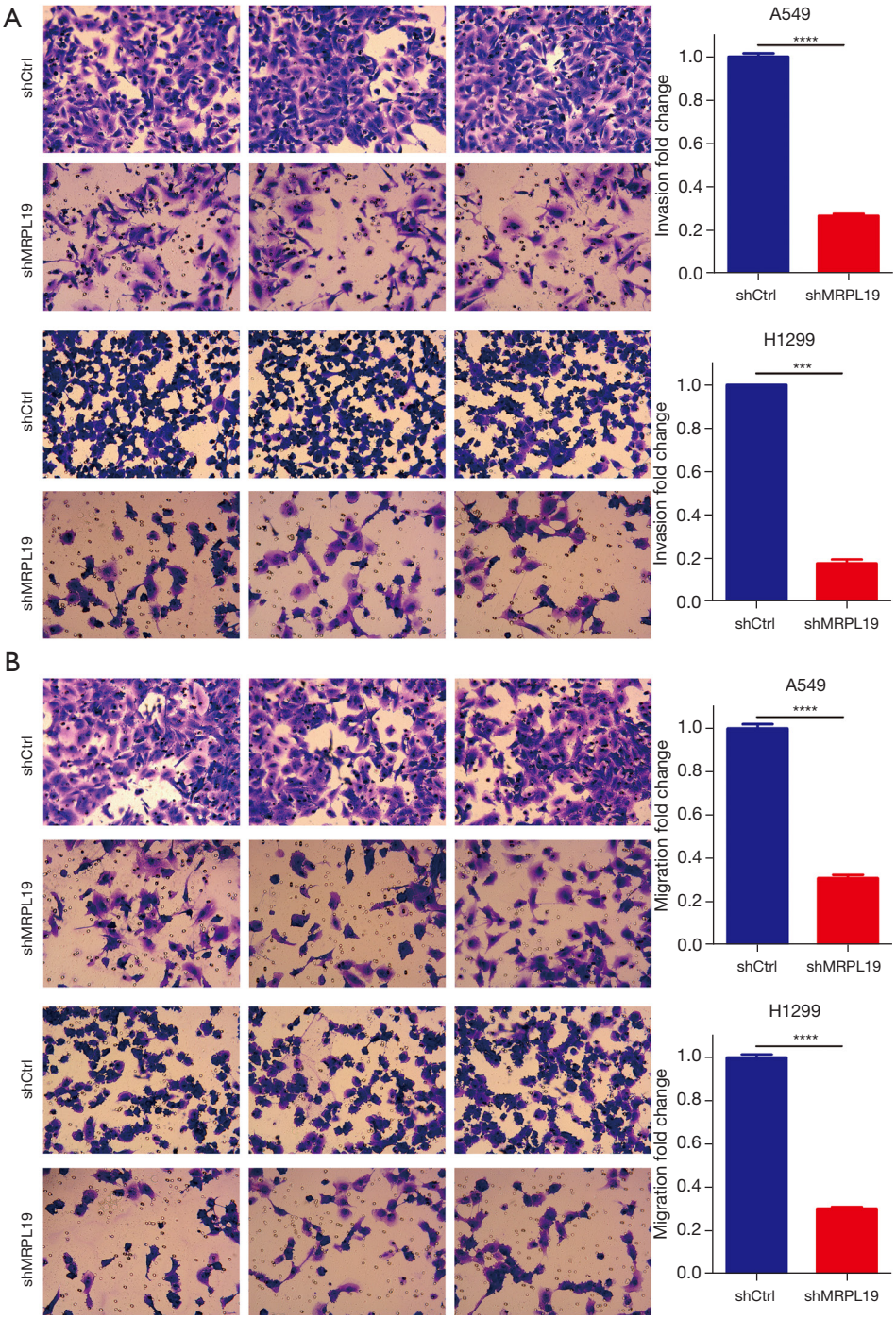

Figure 9 *MRPL19* knockdown suppressed the invasion and migration of LUAD cells. (A) Transwell invasion assay was employed to detect the invasion ability of LUAD cells. (B) Transwell migration assay was employed to detect the migration ability of LUAD cells (Giemsa staining; magnification ×200). ***, P<0.001; ****, P<0.0001. *MRPL19*, mitochondrial ribosomal protein L19; LUAD, lung adenocarcinoma.

tumor-suppressor genes, can lead to the occurrence of lung cancer (27). Cell adhesion molecules have a vital function in epithelial-mesenchymal transition and changes in the tumor microenvironment (TME), both of which are important in the process of tumor cell invasion and migration (28). RNA splicing changes originated by the spliceosome, the catalyst for splicing reactions, have also been potentially involved in the development and/or preservation of cancer (29). Additionally, it has been proposed that an imbalance and switch from Th1 lymphocytes to Th2 phenotype might be crucially linked to the onset and progression of lung cancer, while Th17 cells contribute to antitumor immunity by supporting the aggregation of T cells to the tumor site and the priming of $CD8^+$ T cells. The Th1, Th2, and Th17 lymphocytes are all differentiated from naive $CD4^+$ T cells (30). The gene sets G2M Checkpoint, MYC Targets_V1, MYC Targets_V2, and E2F Targets have been identified by the Molecular Signatures Database (MSigDB) Hallmark as being associated with cell proliferation (31). Uncontrolled growth, genetic instability, and cancer might arise from the proteolytic system being out of regulation as some changes in the ubiquitylation of cell cycle regulators (32). In this regard, the ubiquitin ligase, APC/C, is responsible for the ubiquitin-mediated proteolysis of important cell cycle regulators including cyclins and cyclin-dependent kinase (CDK) suppressors.

Also, mutations and altered gene expression at the mitotic spindle checkpoint have been found to result in aberrant chromosomal content or aneuploidy, which may promote the growth of cancer (33). Therefore, according to our results, it can be inferred that *MRPL19* may exert pro-oncogenic effects in LUAD via pathways connected with cell cycle, cell adhesion molecules, splicing, and mitotic spindle checkpoint. *MRPL19* may also promote the development of LUAD by affecting the tumor immunity.

Kinase, miRNA, and transcription factor target enrichments were performed to investigate the upstream regulators for *MRPL19* dysregulation in LUAD. The outcomes of miRNA-target enrichment indicated that *MRPL19* in LUAD was associated with miR-200A, miR-26A/miR-26B, miR-302C, miR-189, miR-186, and miR-452 expression. In NSCLC cell lines, elevated miR-200A expression encourages growth and migration of cells (34,35). Blocking miR-26a-5p might limit NSCLC cells from proliferating, migrating, and invading, while contributing to their death (36). The development, migration, and invasion of A549 lung malignancy cells *in vitro* along with the development of existing malignancies *in vivo* may be inhibited by the overexpression of miR-26b (37). Additionally, miR-186 elevation significantly diminishes the ability for invasion and migration (38). Therefore, it has been speculated that *MRPL19* may support LUAD proliferation, migration, and invasion with the regulation of miRNAs. In this study, the results of the target transcription factor enrichment showed that *MRPL19* in LUAD was mainly associated with E2F transcription factors. Numerous expressions of genes crucial for cell growth are regulated by the E2F transcription factors (39). In LUAD, a greater expression of E2F family genes was linked to a poor prognosis (40). The outcomes in our study suggest that E2F transcription factors may have a vital function in the modulation of *MRPL19* and may support the growth of LUAD by affecting *MRPL19* expression, but more studies are needed to verify this hypothesis. However, no associated kinase was identified by enrichment analysis.

The TME includes a significant number of immune cells, which have a vital function in the survival and progress of malignancies. An environment that promotes tumor development and metastasis is eventually produced by the interaction between proximal immune cells and cancer cells (41). Thus, the TIMER database was used to investigate the association between *MRPL19* expression and immune cells. The findings demonstrated a substantial negative connotation between *MRPL19* expression and the infiltration of B cells, $CD4^+$ T cells, and dendritic cells. Elevated infiltration of $CD4^+$ T cells or dendritic cells can predict prolonged OS in lung cancer (42,43), which is consistent with the findings of the KM survival curve analysis in this study, which revealed that the low level of infiltration of B cells or dendritic cells could predict poor survival in patients with LUAD. Tumor-infiltrating B cells have been associated with better outcome for patients with lung cancer via the exertion of antitumor immunity (44). The amount of infiltrating B lymphocytes was shown to be an independent prognostic variable in LUAD according to the findings of multivariate Cox regression assessment. Therefore, it is a conceivable hypothesize that *MRPL19* may influence the development of LUAD by modulating the immune cells that infiltrate tumor function.

To confirm the biological role of *MRPL19* in LUAD, associated experiments were performed after *MRPL19* expression was reduced in A549 and H1299 cell lines. The outcomes revealed that the ability for growth, migration, and invasion *in vitro* was reduced after the silencing of *MRPL19*. However, cell apoptosis was not affected after *MRPL19* knockdown. Our experiments further verified the

results of the bioinformatics examination. Therefore, we hypothesized that *MRPL19* might have a pro-oncogenic function in the progression of LUAD.

There are some limitations to the present study. First, the number of clinical specimens in the validation experiment was relatively small, and the sample size should be expanded for a more substantial analysis. Second, the molecular pathways of *MRPL19* in LUAD remain unclear although our investigation did evaluate several functional annotations and included enrichment analysis. Finally, more investigations using other experimental methods should be required to confirm the probable biological mechanisms underlying the relationship between *MRPL19* and the development of LUAD.

Conclusions

Our investigation provides reliable support for the significance of *MRPL19* in the development of LUAD and its potential as a biomarker for LUAD prognosis. Our findings revealed a substantial correlation between increased *MRPL19* expression and the development of LUAD, a poor prognosis, and immune infiltration. Furthermore, our *in vitro* cell results indicate that *MRPL19* may have a pro-oncogenic function in the growth of LUAD.

Acknowledgments

Funding: This work was supported by Hebei Provincial Health Commission Key Science and Technology Research Program (No. 20200552).

Footnote

Reporting Checklist: The authors have completed the MDAR and REMARK reporting checklists. Available at https://tlcr.amegroups.com/article/view/10.21037/tlcr-23-306/rc

Data Sharing Statement: Available at https://tlcr.amegroups.com/article/view/10.21037/tlcr-23-306/dss

Peer Review File: Available at https://tlcr.amegroups.com/article/view/10.21037/tlcr-23-306/prf

Conflicts of Interest: All authors have completed the ICMJE uniform disclosure form (available at https://tlcr.amegroups.com/article/view/10.21037/tlcr-23-306/coif). The authors have no conflicts of interest to declare.

Ethical Statement: The authors are accountable for all aspects of the work in ensuring that questions related to the accuracy or integrity of any part of the work are appropriately investigated and resolved. The study was conducted in accordance with the Declaration of Helsinki (as revised in 2013). The study was approved by the Ethics Committee of the First Affiliated Hospital of Hebei North University (No. W2023012) and informed consent was taken from all the patients.

References

1. Duma N, Santana-Davila R, Molina JR. Non-Small Cell Lung Cancer: Epidemiology, Screening, Diagnosis, and Treatment. Mayo Clin Proc 2019;94:1623-40.
2. Travis WD, Brambilla E, Nicholson AG, et al. The 2015 World Health Organization Classification of Lung Tumors: Impact of Genetic, Clinical and Radiologic Advances Since the 2004 Classification. J Thorac Oncol 2015;10:1243-60.
3. Alexander M, Kim SY, Cheng H. Update 2020: Management of Non-Small Cell Lung Cancer. Lung 2020;198:897-907.
4. Wang M, Herbst RS, Boshoff C. Toward personalized treatment approaches for non-small-cell lung cancer. Nat Med 2021;27:1345-56.
5. Huang G, Li H, Zhang H. Abnormal Expression of Mitochondrial Ribosomal Proteins and Their Encoding Genes with Cell Apoptosis and Diseases. Int J Mol Sci 2020;21:8879.
6. Kim HJ, Maiti P, Barrientos A. Mitochondrial ribosomes in cancer. Semin Cancer Biol 2017;47:67-81.
7. Jing C, Fu R, Wang C, et al. MRPL13 Act as a Novel Therapeutic Target and Could Promote Cell Proliferation in Non-Small Cell Lung Cancer. Cancer Manag Res 2021;13:5535-45.
8. Jiang W, Zhang C, Kang Y, et al. MRPL42 is activated by YY1 to promote lung adenocarcinoma progression. J

Cancer 2021;12:2403-11.
9. Zhang L, Lu P, Yan L, et al. MRPL35 Is Up-Regulated in Colorectal Cancer and Regulates Colorectal Cancer Cell Growth and Apoptosis. Am J Pathol 2019;189:1105-20.
10. Guan X, Zhang H, Qin H, et al. CRISPR/Cas9-mediated whole genomic wide knockout screening identifies mitochondrial ribosomal proteins involving in oxygen-glucose deprivation/reperfusion resistance. J Cell Mol Med 2020;24:9313-22.
11. Wu D, Zhao J, Ma H, et al. Integrating transcriptome-wide association study and copy number variation study identifies candidate genes and pathways for diffuse non-Hodgkin's lymphoma. Cancer Genet 2020;243:7-10.
12. Ayakannu T, Taylor AH, Konje JC. Selection of Endogenous Control Reference Genes for Studies on Type 1 or Type 2 Endometrial Cancer. Sci Rep 2020;10:8468.
13. Christensen JN, Schmidt H, Steiniche T, et al. Identification of robust reference genes for studies of gene expression in FFPE melanoma samples and melanoma cell lines. Melanoma Res 2020;30:26-38.
14. Mohelnikova-Duchonova B, Oliverius M, Honsova E, et al. Evaluation of reference genes and normalization strategy for quantitative real-time PCR in human pancreatic carcinoma. Dis Markers 2012;32:203-10.
15. Ghandi M, Huang FW, Jané-Valbuena J, et al. Next-generation characterization of the Cancer Cell Line Encyclopedia. Nature 2019;569:503-8.
16. Chandrashekar DS, Karthikeyan SK, Korla PK, et al. UALCAN: An update to the integrated cancer data analysis platform. Neoplasia 2022;25:18-27.
17. Vasaikar SV, Straub P, Wang J, et al. LinkedOmics: analyzing multi-omics data within and across 32 cancer types. Nucleic Acids Res 2018;46:D956-63.
18. Zhou Y, Zhou B, Pache L, et al. Metascape provides a biologist-oriented resource for the analysis of systems-level datasets. Nat Commun 2019;10:1523.
19. Li B, Severson E, Pignon JC, et al. Comprehensive analyses of tumor immunity: implications for cancer immunotherapy. Genome Biol 2016;17:174.
20. Sung H, Ferlay J, Siegel RL, et al. Global Cancer Statistics 2020: GLOBOCAN Estimates of Incidence and Mortality Worldwide for 36 Cancers in 185 Countries. CA Cancer J Clin 2021;71:209-49.
21. Bade BC, Dela Cruz CS. Lung Cancer 2020: Epidemiology, Etiology, and Prevention. Clin Chest Med 2020;41:1-24.
22. Schabath MB, Cote ML. Cancer Progress and Priorities: Lung Cancer. Cancer Epidemiol Biomarkers Prev 2019;28:1563-79.
23. Overman RG Jr, Enderle PJ, Farrow JM 3rd, et al. The human mitochondrial translation initiation factor 2 gene (MTIF2): transcriptional analysis and identification of a pseudogene. Biochim Biophys Acta 2003;1628:195-205.
24. Xu D, Wang Y, Wu J, et al. MTIF2 impairs 5 fluorouracil-mediated immunogenic cell death in hepatocellular carcinoma in vivo: Molecular mechanisms and therapeutic significance. Pharmacol Res 2021;163:105265.
25. Pallante P, Forzati F, Federico A, et al. Polycomb protein family member CBX7 plays a critical role in cancer progression. Am J Cancer Res 2015;5:1594-601.
26. Ren J, Yu H, Li W, et al. Downregulation of CBX7 induced by EZH2 upregulates FGFR3 expression to reduce sensitivity to cisplatin in bladder cancer. Br J Cancer 2023;128:232-44.
27. Vincenzi B, Schiavon G, Silletta M, et al. Cell cycle alterations and lung cancer. Histol Histopathol 2006;21:423-35.
28. Janiszewska M, Primi MC, Izard T. Cell adhesion in cancer: Beyond the migration of single cells. J Biol Chem 2020;295:2495-505.
29. Eymin B. Targeting the spliceosome machinery: A new therapeutic axis in cancer? Biochem Pharmacol 2021;189:114039.
30. Duan MC, Zhong XN, Liu GN, et al. The Treg/Th17 paradigm in lung cancer. J Immunol Res 2014;2014:730380.
31. Liberzon A, Birger C, Thorvaldsdóttir H, et al. The Molecular Signatures Database (MSigDB) hallmark gene set collection. Cell Syst 2015;1:417-25.
32. Nakayama KI, Nakayama K. Ubiquitin ligases: cell-cycle control and cancer. Nat Rev Cancer 2006;6:369-81.
33. Sarkar S, Sahoo PK, Mahata S, et al. Mitotic checkpoint defects: en route to cancer and drug resistance. Chromosome Res 2021;29:131-44.
34. Chen Y, Peng W, Lu Y, et al. MiR-200a enhances the migrations of A549 and SK-MES-1 cells by regulating the expression of TSPAN1. J Biosci 2013;38:523-32.
35. Wu X, Liu H, Zhang M, et al. miR-200a-3p promoted cell proliferation and metastasis by downregulating SOX17 in non-small cell lung cancer cells. J Biochem Mol Toxicol 2022;36:e23037.
36. Ye MF, Lin D, Li WJ, et al. MiR-26a-5p Serves as an Oncogenic MicroRNA in Non-Small Cell Lung Cancer by Targeting FAF1. Cancer Manag Res 2020;12:7131-42.
37. Xia M, Duan ML, Tong JH, et al. MiR-26b suppresses tumor cell proliferation, migration and invasion by directly

targeting COX-2 in lung cancer. Eur Rev Med Pharmacol Sci 2015;19:4728-37.
38. Wang J, Zhang Y, Ge F. MiR-186 Suppressed Growth, Migration, and Invasion of Lung Adenocarcinoma Cells via Targeting Dicer1. J Oncol 2021;2021:6217469.
39. Johnson DG, Schneider-Broussard R. Role of E2F in cell cycle control and cancer. Front Biosci 1998;3:d447-8.
40. Wang H, Wang X, Xu L, et al. Integrated analysis of the E2F transcription factors across cancer types. Oncol Rep 2020;43:1133-46.
41. Hinshaw DC, Shevde LA. The Tumor Microenvironment Innately Modulates Cancer Progression. Cancer Res 2019;79:4557-66.
42. Inoshima N, Nakanishi Y, Minami T, et al. The influence of dendritic cell infiltration and vascular endothelial growth factor expression on the prognosis of non-small cell lung cancer. Clin Cancer Res 2002;8:3480-6.
43. Usó M, Jantus-Lewintre E, Bremnes RM, et al. Analysis of the immune microenvironment in resected non-small cell lung cancer: the prognostic value of different T lymphocyte markers. Oncotarget 2016;7:52849-61.
44. Wang SS, Liu W, Ly D, et al. Tumor-infiltrating B cells: their role and application in anti-tumor immunity in lung cancer. Cell Mol Immunol 2019;16:6-18.

(English Language Editor: J. Gray)

Cite this article as: Wei D, Sun D, Sirera R, Afzal MZ, Leong TL, Li X, Wang Y. Overexpression of *MRPL19* in predicting poor prognosis and promoting the development of lung adenocarcinoma. Transl Lung Cancer Res 2023;12(7):1517-1538. doi: 10.21037/tlcr-23-306

Supplementary

Table S1 Signaling pathways were showed in PPI network

MCODE	GO	Description	Log10(P)
MCODE_1	R-HSA-174184	Cdc20:Phospho-APC/C mediated degradation of Cyclin A	-15.3
MCODE_1	R-HSA-179419	APC:Cdc20 mediated degradation of cell cycle proteins prior to satisfation of the cell cycle checkpoint	-15.2
MCODE_1	R-HSA-176409	APC/C:Cdc20 mediated degradation of mitotic proteins	-15.1
MCODE_2	GO:0051052	Regulation of DNA metabolic process	-9.2
MCODE_2	CORUM:2224	MSH2/6-BLM-p53-RAD51 complex	-8.4
MCODE_2	R-HSA-73894	DNA Repair	-8.2
MCODE_3	GO:0019886	Antigen processing and presentation of exogenous peptide antigen via MHC class II	-8.2
MCODE_3	GO:0002495	Antigen processing and presentation of peptide antigen via MHC class II	-8.1
MCODE_3	GO:0002504	Antigen processing and presentation of peptide or polysaccharide antigen via MHC class II	-8.1
MCODE_4	GO:0034470	ncRNA processing	-14.2
MCODE_4	GO:0034660	ncRNA metabolic process	-13.5
MCODE_4	GO:0006364	rRNA processing	-13.5
MCODE_5	R-HSA-72163	mRNA Splicing - Major Pathway	-13.3
MCODE_5	R-HSA-72172	mRNA Splicing	-13.2
MCODE_5	R-HSA-72203	Processing of Capped Intron-Containing Pre-mRNA	-12.6
MCODE_6	R-HSA-141444	Amplification of signal from unattached kinetochores via a MAD2 inhibitory signal	-7.5
MCODE_6	R-HSA-141424	Amplification of signal from the kinetochores	-7.5
MCODE_6	R-HSA-69618	Mitotic Spindle Checkpoint	-7.3
MCODE_7	GO:0006520	Cellular amino acid metabolic process	-6.1

https://dx.doi.org/10.21037/tlcr-23-306